

# Trigon Robotic Pairs

A. Scott Howe, PhD<sup>\*</sup>  
*Plug-in Creations Architecture, LLC*  
*Hong Kong University Dept. of Architecture*

Ian Gibson, PhD.<sup>†</sup>  
*National University of Singapore Dept. of Mechanical Engineering*

**The Trigon modular robotic construction system consists of square or equilateral triangle panels that are able to grasp each other at edge points to affect self-assembly. The Trigon system can be used to construct a variety of stable geometries and structures for habitats and vehicles, including rovers, ISRU “cassette factories”, and permanent base structures. Construction is accomplished by panel pairs that use each other to “tumble” across completed portions of the structure until they find their target positions. This paper discusses robotic pair kinematics and inverse kinematics, assembly sequences, and preliminary robot prototypes.**

## I. Introduction

This paper describes the kinematics for the Transformable Robotic Infrastructure-Generating Object Network (Trigon) modular robotic construction system. Two panel types are described herein, namely triangle and square panels. It is assumed there are two ways a set of panels can be used to assemble a specified enclosure:

1. Unfolding: Each panel in the set has limited connection with the others, just enough to allow the entire set to be folded into a compact form. At the time of deployment, the package then “unfurls” and the remaining connections between panels are made to fill out the target geometry.
2. Assembly: Panels are added to the completed structure incrementally and autonomously make their way across the structure to their assigned location for insertion. Studies with simulations and mockups have shown that panels must work in pairs to complete the task of relocation across existing structure.

This paper refers to equations describing the configurations, processes, and sequences required in the above (2) assembly task, across a completed structure of panels consisting of the same geometry as those in motion (triangles across triangles, squares across squares). Initially the panels are described diagrammatically, showing parameters, dependencies, and geometrical equations. Diagrams include geometric constraints and descriptions, and kinematic equivalents. Equations are defined for degree of freedom, forward / reverse kinematic analysis, and torque under different gravity accelerations.

## II. Panel Geometries

The Trigon concept consists of panels that mechanically connect at their edges (Figure 1). Connections are simplified by avoiding joints at the vertices, so all relationships are planar revolute. With this simple connection protocol, the equilateral triangles and squares can be assembled into a variety of stable, useful geometries. However, in the current stage of development, optimum panel edge dimensions, mechanism sizes, and panel thicknesses are still unknown. In a parallel study, a program has been developed that rigorously explores the effect that panel edge length has on mechanism sizes and torque (Howe, Gibson 2006b). The geometry equations will allow a parametric approach that will aid in the selection of mechanisms, which may determine the other dimensions. Howe and Gibson (2006b) describe Triangle and square panels with all their parameters and dependencies.

---

<sup>\*</sup> Assistant Professor, HKU Department of Architecture, ash@plugin-creations.com, AIAA member

<sup>†</sup> Associate Professor, NUS Department of Mechanical Engineering, mpegi@nus.edu.sg

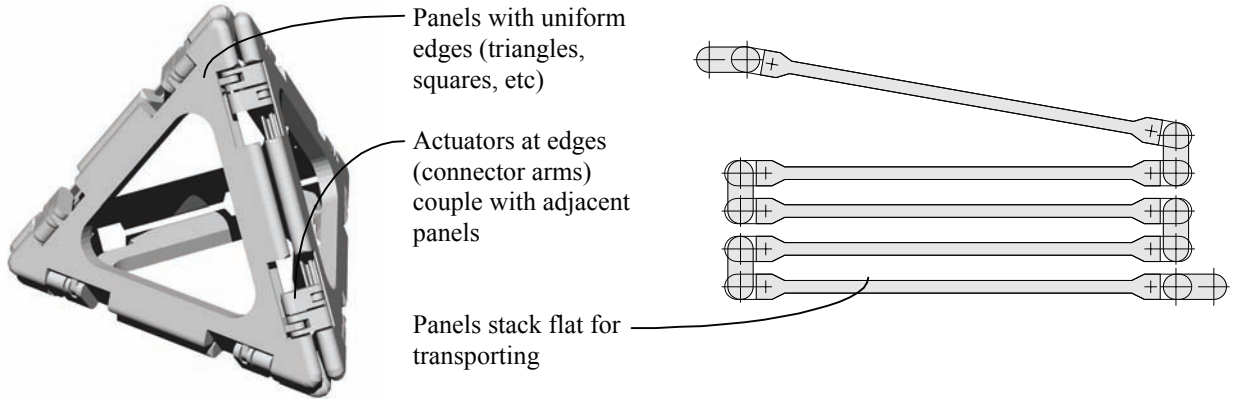
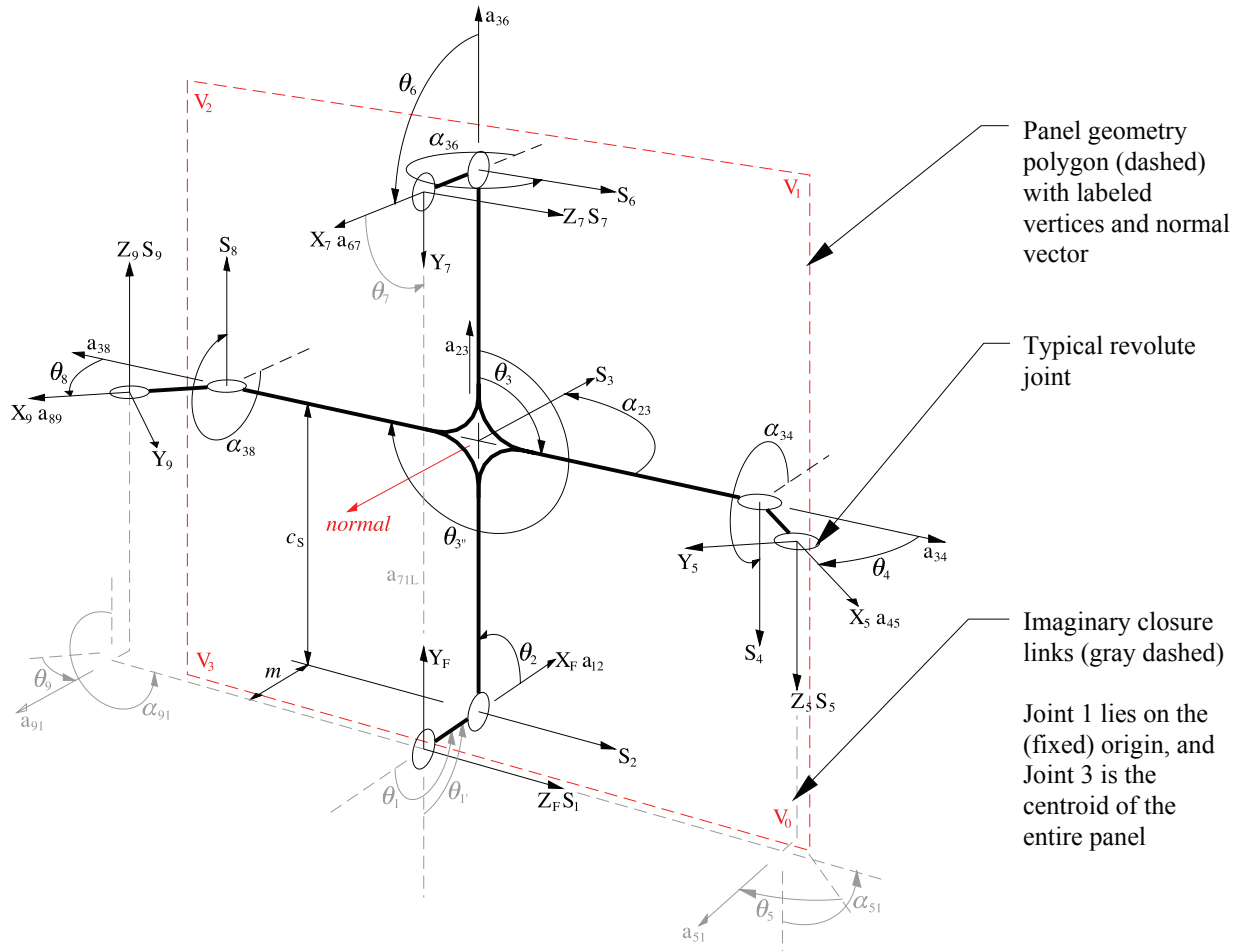


Figure 1: Trigon panel concept (triangular panel shown)



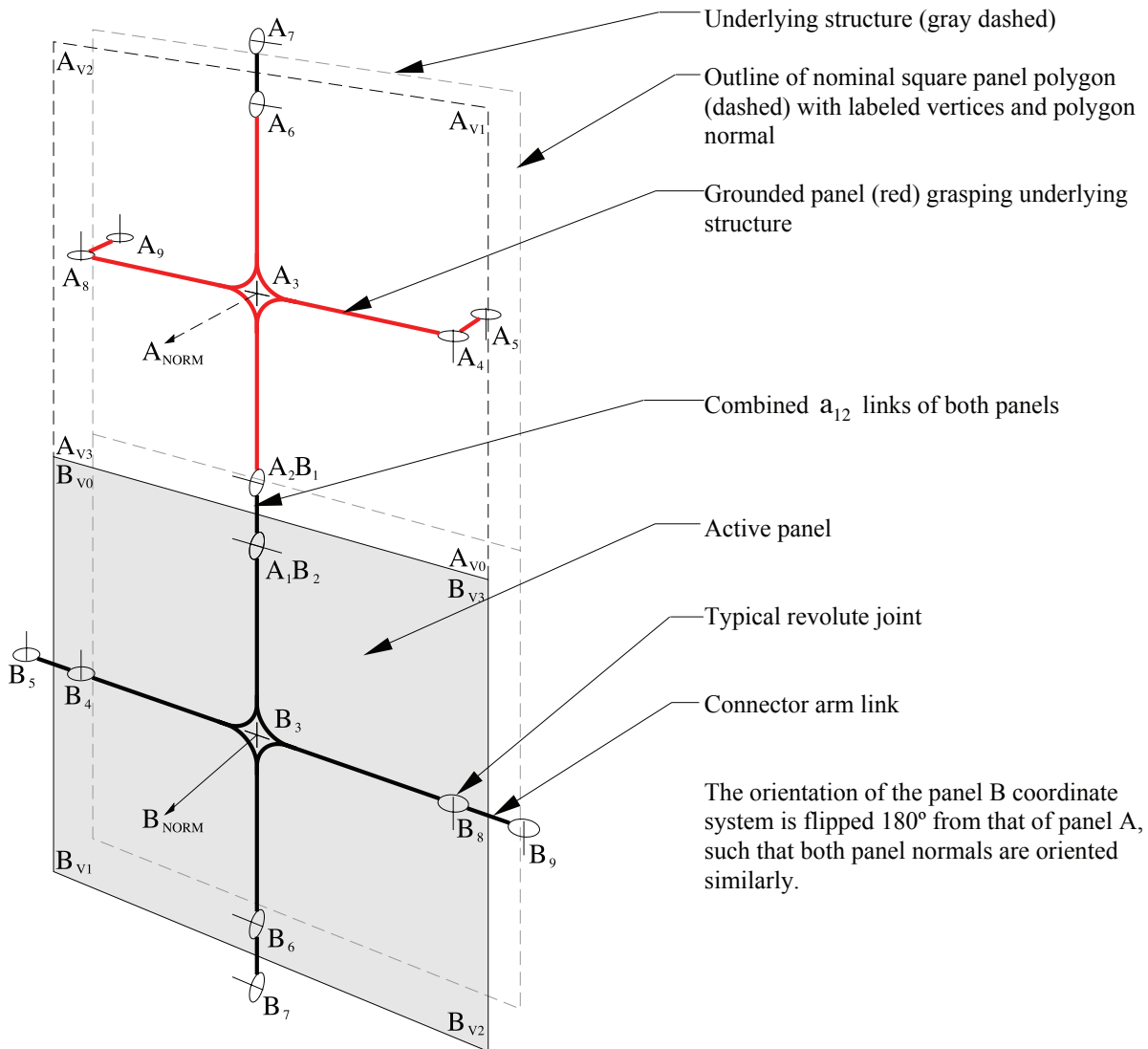
$c_S =$  distance to centroid,  $m =$  connector manipulator arm length  
 $\theta_1 = 270 - \theta_2$ ,  $\theta_5 = 90 - \theta_4$ ,  $\theta_7 = 720 - \theta_1 - \theta_2 - \theta_6$ ,  $\theta_9 = 90 - \theta_8$   
 $a_{51} = -a_{12} \sin \theta_2 + a_{45} \sin \theta_4$ ,  $a_{91} = -a_{12} \sin \theta_2 + a_{89} \sin \theta_8$   
 $a_{71} = \sqrt{(a_{12} \sin \theta_2 - a_{67} \sin \theta_6)^2 + (a_{12} \cos \theta_2 + 2c_S + a_{67} \cos \theta_6)^2}$   
 $S_1 = c_S + a_{45} \cos \theta_4$ ,  $S_{1''} = c_S + a_{89} \cos \theta_8$ ,  $S_5 = S_9 = c_S + a_{12} \cos \theta_2$

Figure 2: Square panel kinematic diagram

### III. Panel Kinematics

At each edge, a pair of connector arms function in tandem as manipulators, to grasp or be grasped by a neighboring panel. For kinematic functionality purposes, pairs of connector arms at each edge can be combined into an equivalent single link, where the panel bodies can be represented as ternary links or quaternary links. In the following diagrams, each panel has been simplified so that the ternary and quaternary elements consist of serial branched elements that pass through the panel centroid fixed joint. Connector arms are assumed to be single links, where double manipulator arm pairs are ignored. The diagram in Figure 2 uses the Denavit-Hartenberg method for labeling (Crane & Duffy 1998, p28).

In practical applications, previous studies have shown that the panels must work in pairs to navigate across structure already in place. Therefore, the actual functional robotic mechanism would consist of panel pairs. The kinematic diagram for square panel pairs is shown in Figure 3. The pairs are created by clasping the connector arm links  $a_{12}$  from both panels (A and B) for the purpose of combining them into a single link.



**Figure 3: Square panel robotic pair**

When panels are added to the structure incrementally, robotic pairs of panels shown in Figure 3 are placed onto an existing portion of the structure (the method for placement of the pair onto the structure will not be discussed within

the scope of this paper). Figure 4 through Figure 8 show the climbing sequence scenario of a square panel robotic pair across similar square panels pre-existing in an underlying wall (the triangle pair climbing sequence is similar). The sequence is depicted as a vertical upward climb, which is assumed to be the most difficult. Subsequently, kinematic and dynamic analyses will be performed using this scenario.

The climbing sequence scenario is as follows:

Step 1: Robotic panel pair is attached to a wall consisting of pre-existing panels that have been inserted into the structure previously (Figure 4). Connector arm Joints  $B_5$  and  $B_9$  grasp onto points  $D_4$  and  $D_8$  of underlying panel D. At this stage Panel B becomes grounded, leaving joint  $A_1B_2$  free for movement, along with all the joints on Panel A. Robotic pair joint parameters for Step 1 are:

$$\begin{aligned}\theta_{A2} &= 90 & \theta_{B2} &= 90 \\ \theta_{A4} &= -90 & \theta_{B4} &= -90 \\ \theta_{A6} &= 0 & \theta_{B6} &= 0 \\ \theta_{A8} &= -90 & \theta_{B8} &= -90\end{aligned}$$

Step 2: The polygon normals of Panel B and target Panel C are evaluated to determine the (faceted) curvature of the underlying structure. If the normals are parallel, revolute actuators at Joint  $A_1B_2$  lift Panel A 90 degrees to cantilever out from the wall (Figure 5). A discussion will be made later about assembly sequence in the case of non-parallel polygon normals. Robotic pair joint parameters for Step 2 are:

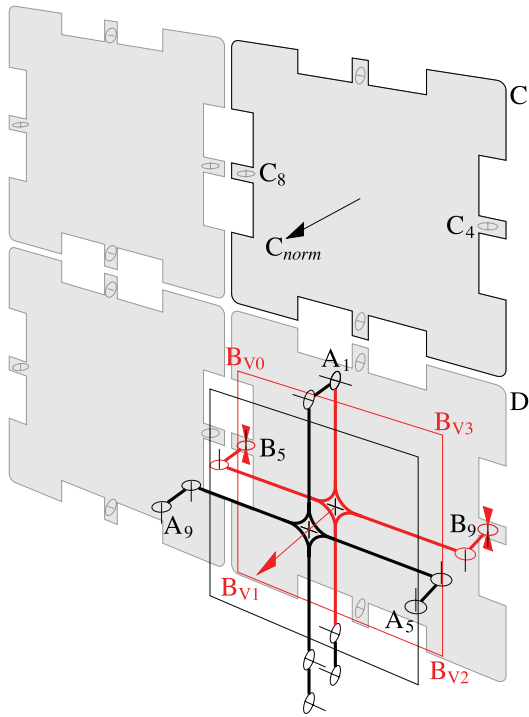
$$\begin{aligned}\theta_{A2} &= 90 & \theta_{B2} &= 0 \\ \theta_{A4} &= -90 & \theta_{B4} &= -90 \\ \theta_{A6} &= 0 & \theta_{B6} &= 0 \\ \theta_{A8} &= -90 & \theta_{B8} &= -90\end{aligned}$$

Step 3: Revolute actuators at Joint  $A_2B_1$  continue to lift Panel A 90 degrees until connector arm Joints  $A_5$  and  $A_9$  can grasp onto points  $C_4$  and  $C_8$  on the underlying wall Panel C (Figure 6). At this stage the entire robot pair is grounded, excepting the unused hanging Joints  $A_7$  and  $B_7$  at the top and bottom of the mechanism. Robotic pair joint parameters for Step 3 are:

$$\begin{aligned}\theta_{A2} &= 0 & \theta_{B2} &= 0 \\ \theta_{A4} &= -90 & \theta_{B4} &= -90 \\ \theta_{A6} &= 0 & \theta_{B6} &= 0 \\ \theta_{A8} &= -90 & \theta_{B8} &= -90\end{aligned}$$

Step 4: Once Joints  $A_5$  and  $A_9$  have securely grasped the underlying wall panel, Joints  $B_5$  and  $B_9$  can release their grasp. Revolute actuators at Joint  $A_1B_2$  will then lift Panel B 90 degrees to cantilever out from the wall (Figure 7). Robotic pair joint parameters for Step 4 are:

$$\begin{aligned}\theta_{A2} &= 0 & \theta_{B2} &= 90 \\ \theta_{A4} &= -90 & \theta_{B4} &= -90 \\ \theta_{A6} &= 0 & \theta_{B6} &= 0 \\ \theta_{A8} &= -90 & \theta_{B8} &= -90\end{aligned}$$



Gray panels show pre-existing underlying wall, consisting of panels that have been inserted into the structure previously

Points  $C_8$  and  $C_4$  on underlying Panel C, are waiting to receive connector arms  $A_5$  and  $A_9$  of climbing Panel A

Grounded portion of robotic pair is shown in red.

Figure 4: Panel climbing sequence step 1

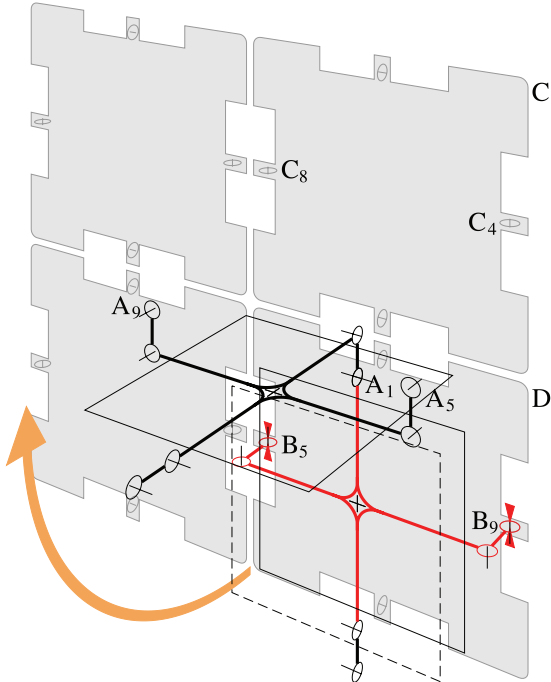


Figure 5: Panel climbing sequence step 2

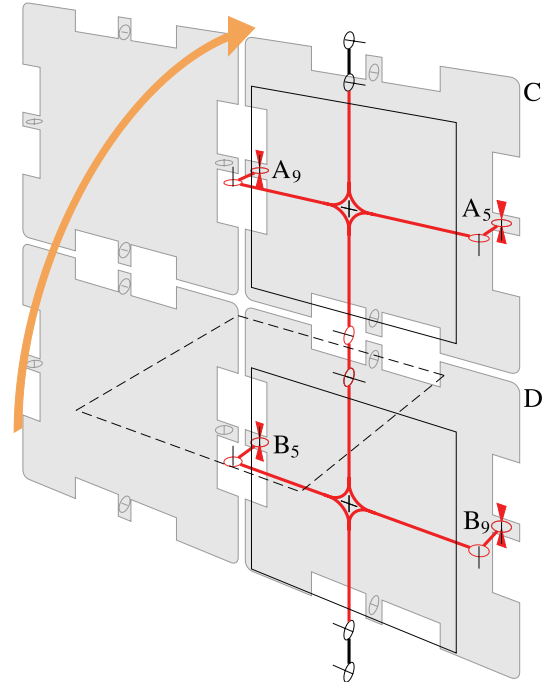


Figure 6: Panel climbing sequence step 3

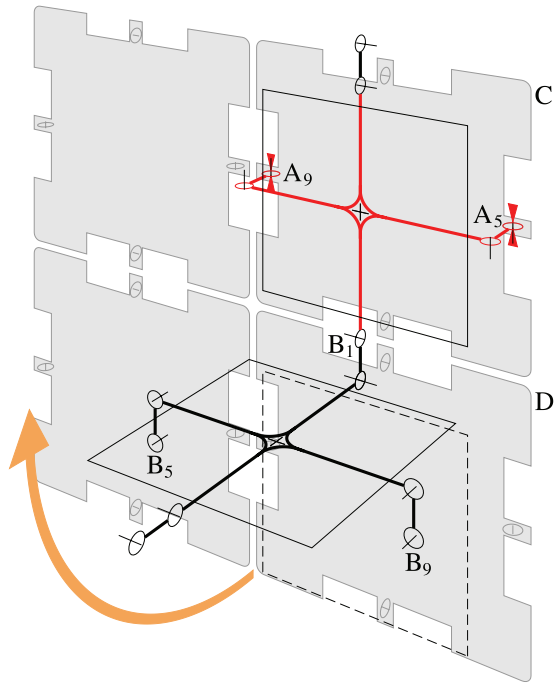


Figure 7: Panel climbing sequence step 4

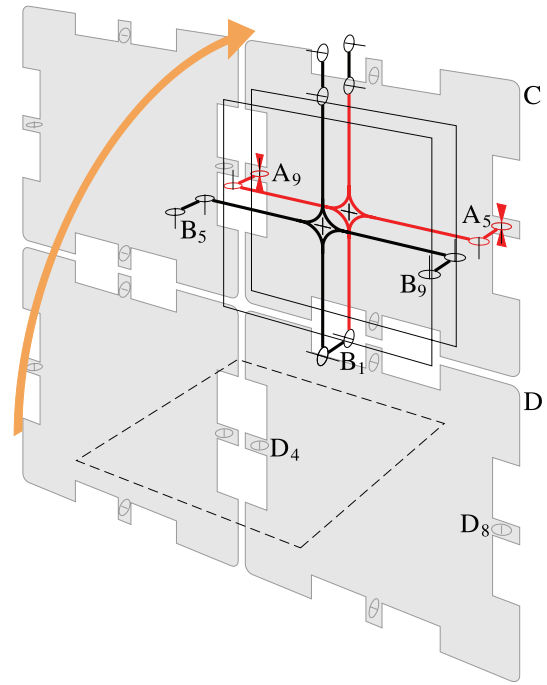


Figure 8: Panel climbing sequence step 5

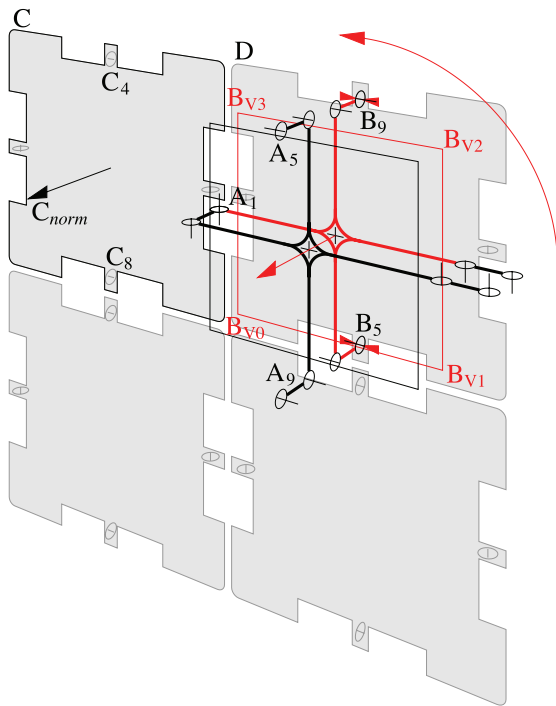


Figure 9: Remapping joint notation

When the route of travel changes direction, joints reconfigure themselves in the new orientation

Panel polygon vertices, joint notation, and assembly sequence remaps itself onto the new orientation

Step 5: Revolute actuators at Joint  $A_2B_1$  continue to lift Panel B 90 degrees until Panels A and B are back-to-back again (Figure 8). Robotic pair joint parameters for Step 5 are:

$$\begin{aligned} \theta_{A_2} &= 90 & \theta_{B_2} &= 90 \\ \theta_{A_4} &= -90 & \theta_{B_4} &= -90 \\ \theta_{A_6} &= 0 & \theta_{B_6} &= 0 \\ \theta_{A_8} &= -90 & \theta_{B_8} &= -90 \end{aligned}$$

At this stage, the next target position is determined. If the pair is to continue the upward climb, Joints  $A_6$  and  $A_7$  can mate with Joints  $B_6$  and  $B_7$ , and Joints  $A_1$  and  $A_2$  can release points  $B_2$  and  $B_1$ , bringing the robotic pair back to the exact configuration described in Step 1, where all joint notation is remapped to the new starting position. New remappings  $A'$  and  $B'$  would be (the symbol “>” means “maps to”):

$$\begin{aligned} A_1 &> B'_7 & A_6 &> B'_2 & B_1 &> A'_7 & B_6 &> A'_2 \\ A_2 &> B'_6 & A_7 &> B'_1 & B_2 &> A'_6 & B_7 &> A'_1 \\ A_3 &> B'_3 & A_8 &> B'_4 & B_3 &> A'_3 & B_8 &> A'_4 \\ A_4 &> B'_8 & A_9 &> B'_5 & B_4 &> A'_8 & B_9 &> A'_5 \\ A_5 &> B'_9 & & & B_5 &> A'_9 & & \end{aligned}$$

Alternatively, the robotic pair can reorient itself 90 degrees in order to travel to the right or left, with a remapping of the labels and joint notation (Figure 9). New remappings  $A'$  and  $B'$  right and left would be:

Right				Left			
$A_1 > B'_9$	$A_6 > B'_4$	$B_1 > A'_5$	$B_6 > A'_8$	$A_1 > B'_5$	$A_6 > B'_8$	$B_1 > A'_9$	$B_6 > A'_4$
$A_2 > B'_8$	$A_7 > B'_5$	$B_2 > A'_4$	$B_7 > A'_9$	$A_2 > B'_4$	$A_7 > B'_9$	$B_2 > A'_8$	$B_7 > A'_5$
$A_3 > B'_3$	$A_8 > B'_6$	$B_3 > A'_3$	$B_8 > A'_2$	$A_3 > B'_3$	$A_8 > B'_2$	$B_3 > A'_3$	$B_8 > A'_6$
$A_4 > B'_2$	$A_9 > B'_7$	$B_4 > A'_6$	$B_9 > A'_1$	$A_4 > B'_6$	$A_9 > B'_1$	$B_4 > A'_2$	$B_9 > A'_7$
$A_5 > B'_1$		$B_5 > A'_7$		$A_5 > B'_7$		$B_5 > A'_1$	

### A. Forward Kinematics for Square panels

The square panels consist of a kinematic chain with three branches. In order to find a solution for climbing square panels, forward kinematic analysis of the two side branches are required. Analysis of the center branch is also required in some situations. As with the triangle panels, the three branch chains are coincident up to Joint 3, whereupon the split occurs. Table 1 shows the mechanism parameters that will be used in the analysis (see Figure 2).

Link length	Twist angle	Joint offset	Joint angle	Joint range
$a_{12} = m$	$\alpha_{12} = 0$	$S_1 = \text{variable}$	$\theta_1 = \text{variable}$	
$a_{23} = c_s$	$\alpha_{23} = 90$	$S_2 = 0$	$\theta_2 = \text{variable}$	-90 to 90
$a_{34} = c_s$	$\alpha_{34} = 270$	$S_3 = 0$	$\theta_3 = 90$	
$a_{45} = m$	$\alpha_{45} = 0$	$S_4 = 0$	$\theta_4 = \text{variable}$	-90 to 90
$a_{51} = \text{variable}$	$\alpha_{51} = 90$	$S_5 = \text{variable}$	$\theta_5 = \text{variable}$	
$a_{36} = c_s$	$\alpha_{36} = 270$	$S_3 = 0$	$\theta_{3'} = 0$	
$a_{67} = m$	$\alpha_{67} = 0$	$S_6 = 0$	$\theta_6 = \text{variable}$	-90 to 90
$a_{71} = \text{variable}$	$\alpha_{71} = 0$	$S_7 = 0$	$\theta_7 = \text{variable}$	
$a_{38} = c_s$	$\alpha_{38} = 270$	$S_3 = 0$	$\theta_{3'} = 270$	
$a_{89} = m$	$\alpha_{89} = 0$	$S_8 = 0$	$\theta_8 = \text{variable}$	-90 to 90
$a_{91} = \text{variable}$	$\alpha_{91} = 270$	$S_9 = \text{variable}$	$\theta_9 = \text{variable}$	

**Table 1: Square panel mechanism parameters**

3x3 orientation matrices are used in combination with a 3x1 position matrix, embedded in a 4x4 transformation matrix (Tsai 1999, p37). The Denavit-Hartenberg method as presented by Crane & Duffy (1998) utilizes only the Z and X axis for the local coordinate systems (for  $\theta$  and  $\alpha$  respectively). Simplifying the equations to take into account 0 or 1 values for twist angle  $\alpha$ , the forward kinematic homogeneous transformation matrices for the two side branches of a square panel are ( ${}^1_2T_S$  are common to SRB = “Square Right Branch”, SLB = “Square Left Branch”, and SMB = “Square Middle Branch”):

$${}^1_2T_S = \begin{bmatrix} \cos\theta_2 & -\sin\theta_2 & 0 & a_{12} \\ \sin\theta_2 & \cos\theta_2 & 0 & 0 \\ 0 & 0 & 1 & 0 \\ 0 & 0 & 0 & 1 \end{bmatrix}$$

$${}^2_3T_{SRB} = \begin{bmatrix} 0 & -1 & 0 & a_{23} \\ 0 & 0 & -1 & 0 \\ 1 & 0 & 0 & 0 \\ 0 & 0 & 0 & 1 \end{bmatrix} \quad {}^2_{3'}T_{SLB} = \begin{bmatrix} 0 & 1 & 0 & a_{23} \\ 0 & 0 & -1 & 0 \\ -1 & 0 & 0 & 0 \\ 0 & 0 & 0 & 1 \end{bmatrix}$$

$${}^3_4T_{SRB} = \begin{bmatrix} \cos\theta_4 & -\sin\theta_4 & 0 & a_{34} \\ 0 & 0 & 1 & 0 \\ -\sin\theta_4 & -\cos\theta_4 & 0 & 0 \\ 0 & 0 & 0 & 1 \end{bmatrix} \quad {}^3_8T_{SLB} = \begin{bmatrix} \cos\theta_8 & -\sin\theta_8 & 0 & a_{38} \\ 0 & 0 & 1 & 0 \\ -\sin\theta_8 & -\cos\theta_8 & 0 & 0 \\ 0 & 0 & 0 & 1 \end{bmatrix}$$

$${}^4_5T_{SRB} = \begin{bmatrix} 1 & 0 & 0 & a_{45} \\ 0 & 1 & 0 & 0 \\ 0 & 0 & 1 & 0 \\ 0 & 0 & 0 & 1 \end{bmatrix} \quad {}^8_9T_{SLB} = \begin{bmatrix} 1 & 0 & 0 & a_{89} \\ 0 & 1 & 0 & 0 \\ 0 & 0 & 1 & 0 \\ 0 & 0 & 0 & 1 \end{bmatrix}$$

And the forward kinematic homogeneous transformation matrices for the middle branch SMB of a square panel are:

$${}^2_{3'}T_{SMB} = \begin{bmatrix} 1 & 0 & 0 & a_{23} \\ 0 & 0 & -1 & 0 \\ 0 & 1 & 0 & 0 \\ 0 & 0 & 0 & 1 \end{bmatrix}$$

$${}^3_6T_{SMB} = \begin{bmatrix} \cos\theta_6 & -\sin\theta_6 & 0 & a_{36} \\ 0 & 0 & 1 & 0 \\ -\sin\theta_6 & -\cos\theta_6 & 0 & 0 \\ 0 & 0 & 0 & 1 \end{bmatrix}$$

$${}^6_7\mathbf{T}_{\text{SMB}} = \begin{bmatrix} 1 & 0 & 0 & a_{67} \\ 0 & 1 & 0 & 0 \\ 0 & 0 & 1 & 0 \\ 0 & 0 & 0 & 1 \end{bmatrix}$$

In the middle branch, the equation for  $\theta_1$ , needs to be modified as follows:

$$\sin \theta_1 = \frac{\sin \theta_2 (a_{23} + a_{36}) + a_{67} \sin(\theta_2 + \theta_6)}{a_{71}} \quad \cos \theta_1 = \frac{a_{12} + \cos \theta_2 (a_{23} + a_{36}) + a_{67} \cos(\theta_2 + \theta_6)}{-a_{71}}$$

Therefore  $\theta_1 = \text{Atan2}(\sin \theta_1, \cos \theta_1)$

Transformations relating the end effector coordinate systems of the side branches  ${}^1_5\mathbf{T}_{\text{SRB}}$  and  ${}^1_9\mathbf{T}_{\text{SLB}}$  with the fixed coordinate system are shown as follows:

$${}^1_5\mathbf{T}_{\text{SRB}} = {}^1_2\mathbf{T}_S {}^2_3\mathbf{T}_{\text{SRB}} {}^3_4\mathbf{T}_{\text{SRB}} {}^4_5\mathbf{T}_{\text{SRB}}$$

$${}^1_9\mathbf{T}_{\text{SLB}} = {}^1_2\mathbf{T}_S {}^2_3\mathbf{T}_{\text{SLB}} {}^3_8\mathbf{T}_{\text{SLB}} {}^8_9\mathbf{T}_{\text{SLB}}$$

The transformation of the middle branch  ${}^1_7\mathbf{T}_{\text{SMB}}$  is as follows:

$${}^1_7\mathbf{T}_{\text{SMB}} = {}^1_2\mathbf{T}_S {}^2_3\mathbf{T}_{\text{SMB}} {}^3_6\mathbf{T}_{\text{SMB}} {}^6_7\mathbf{T}_{\text{SMB}}$$

As with the triangle panels, positions of Joints 5, 9, and 7 can be calculated, along with any other joint using continuous strings of transformation matrices.

## B. Inverse Kinematics for Square Panels

The inverse of a homogeneous transformation matrix consists of swapping rows and columns of the 3x3 orientation matrix in the forward transformation matrix, and using the dot product of the three orientation vectors on the position vector (Paul, Shimano, Mayer 1981, p72). Using the imaginary closure link shown in gray in Figure 2 (with parameters shown in light blue in Table 1), two sets of equations can be derived for the square panels. The final transformation  ${}^5_1\mathbf{T}_{\text{SRB}}$  (back to origin) of the right branch SRB of the square panel is as follows:

$${}^5_1\mathbf{T}_{\text{SRB}} = \begin{bmatrix} c\theta_1 c\theta_5 - s\theta_1 s\theta_5 c\alpha_{51} & -s\theta_1 c\theta_5 - c\theta_1 s\theta_5 c\alpha_{51} & s\theta_5 s\alpha_{51} & a_{51} c\theta_5 - S_1 s\theta_5 s\alpha_{51} \\ c\theta_1 s\theta_5 + s\theta_1 c\theta_5 c\alpha_{51} & -s\theta_1 s\theta_5 + c\theta_1 c\theta_5 c\alpha_{51} & -c\theta_5 s\alpha_{51} & a_{51} s\theta_5 + S_1 c\theta_5 s\alpha_{51} \\ s\theta_1 s\alpha_{51} & c\theta_1 s\alpha_{51} & c\alpha_{51} & -S_1 c\alpha_{51} + S_5 \\ 0 & 0 & 0 & 1 \end{bmatrix}$$

The inverse  ${}^1_5\mathbf{R}_{\text{SRB}}$  of  ${}^5_1\mathbf{T}_{\text{SRB}}$  is as follows:

$${}^1_5\mathbf{R}_{SRB} = \begin{bmatrix} c\theta_1 c\theta_5 - s\theta_1 s\theta_5 c\alpha_{51} & c\theta_1 s\theta_5 + s\theta_1 c\theta_5 c\alpha_{51} & s\theta_1 s\alpha_{51} & -a_{51} c\theta_1 + S_5 s\theta_1 s\alpha_{51} \\ -s\theta_1 c\theta_5 - c\theta_1 s\theta_5 c\alpha_{51} & -s\theta_1 s\theta_5 + c\theta_1 c\theta_5 c\alpha_{51} & c\theta_1 s\alpha_{51} & -a_{51} s\theta_1 - S_5 c\theta_1 s\alpha_{51} \\ s\theta_5 s\alpha_{51} & -c\theta_5 s\alpha_{51} & c\alpha_{51} & S_1 - S_5 c\alpha_{51} \\ 0 & 0 & 0 & 1 \end{bmatrix}$$

Using the vector elements from the right branch SRB, we can find the angles for the square right branch in the following order:

$$\theta_{1SRB} = \text{Atan2}\left(\frac{w_{xSRB}}{\sin\alpha_{51}}, \frac{w_{ySRB}}{\sin\alpha_{51}}\right)$$

$$\theta_{2SRB} = \text{Atan2}(-w_{ySRB}, -w_{xSRB})$$

$$\theta_{5SRB} = \text{Atan2}\left(\frac{u_{zSRB}}{\sin\alpha_{51}}, \frac{-u_{xSRB} - u_{ySRB} \sin\theta_1 \cos\alpha_{51}}{\cos\alpha_{51}(\sin^2\theta_1 + \cos^2\theta_1)}\right)$$

$$\theta_{4SRB} = \text{Atan2}\left(\cos\theta_5 \sin\alpha_{51}, \frac{q_{zSRB} - a_{34}}{a_{45}}\right)$$

Similarly, we can find the angles for the square left branch in the following order:

$$\theta_{1SLB} = \text{Atan2}\left(\frac{w_{xSLB}}{\sin\alpha_{91}}, \frac{w_{ySLB}}{\sin\alpha_{91}}\right)$$

$$\theta_{2SLB} = \text{Atan2}(w_{ySLB}, w_{xSLB})$$

$$\theta_{9SLB} = \text{Atan2}\left(\frac{u_{zSLB}}{\sin\alpha_{91}}, \frac{-u_{xSLB} - u_{ySLB} \sin\theta_1 \cos\alpha_{91}}{\cos\alpha_{91}(\sin^2\theta_1 + \cos^2\theta_1)}\right)$$

$$\theta_{8SLB} = \text{Atan2}\left(-\cos\theta_9 \sin\alpha_{91}, \frac{-q_{zSLB} - a_{38}}{a_{89}}\right)$$

And middle branch:

$$\theta_{2SMB} = \text{Atan2}\left(\frac{q_{xSMB} - a_{12} - a_{67}u_{xSMB}}{a_{23} + a_{36}}, \frac{q_{ySMB} - a_{67}u_{ySMB}}{a_{23} + a_{36}}\right)$$

$$\theta_{6SMB} = \text{Atan2}\left(\frac{u_{ySMB} \cos\theta_2 - u_{xSMB} \sin\theta_2}{\sin^2\theta_2 + \cos^2\theta_2}, \frac{u_{ySMB} \sin\theta_2 + u_{xSMB} \cos\theta_2}{\sin^2\theta_2 + \cos^2\theta_2}\right)$$

$$\theta_{1'SMB} = \text{Atan2} \left( \frac{q_{ySMB} (q_{ySMB} u_{xSMB} + u_{ySMB})}{q_{ySMB}^2 - q_{xSMB}}, \frac{q_{xSMB} (q_{ySMB} u_{xSMB} + u_{ySMB})}{q_{ySMB}^2 - q_{xSMB}} \right)$$

$$\theta_{7SMB} = \text{Atan2} \left( \frac{u_{ySMB} \cos \theta_1 - u_{xSMB} \sin \theta_1}{\sin^2 \theta_1 + \cos^2 \theta_1}, \frac{u_{ySMB} \sin \theta_1 + u_{xSMB} \cos \theta_1}{\sin^2 \theta_1 + \cos^2 \theta_1} \right)$$

The geometry equations, and forward and inverse kinematics equations have been modeled in MatLab for simulation. Figure 10 shows a software control panel for inputting joint angles of triangle panels, where the output is the resulting vector and position of the free connector arms.

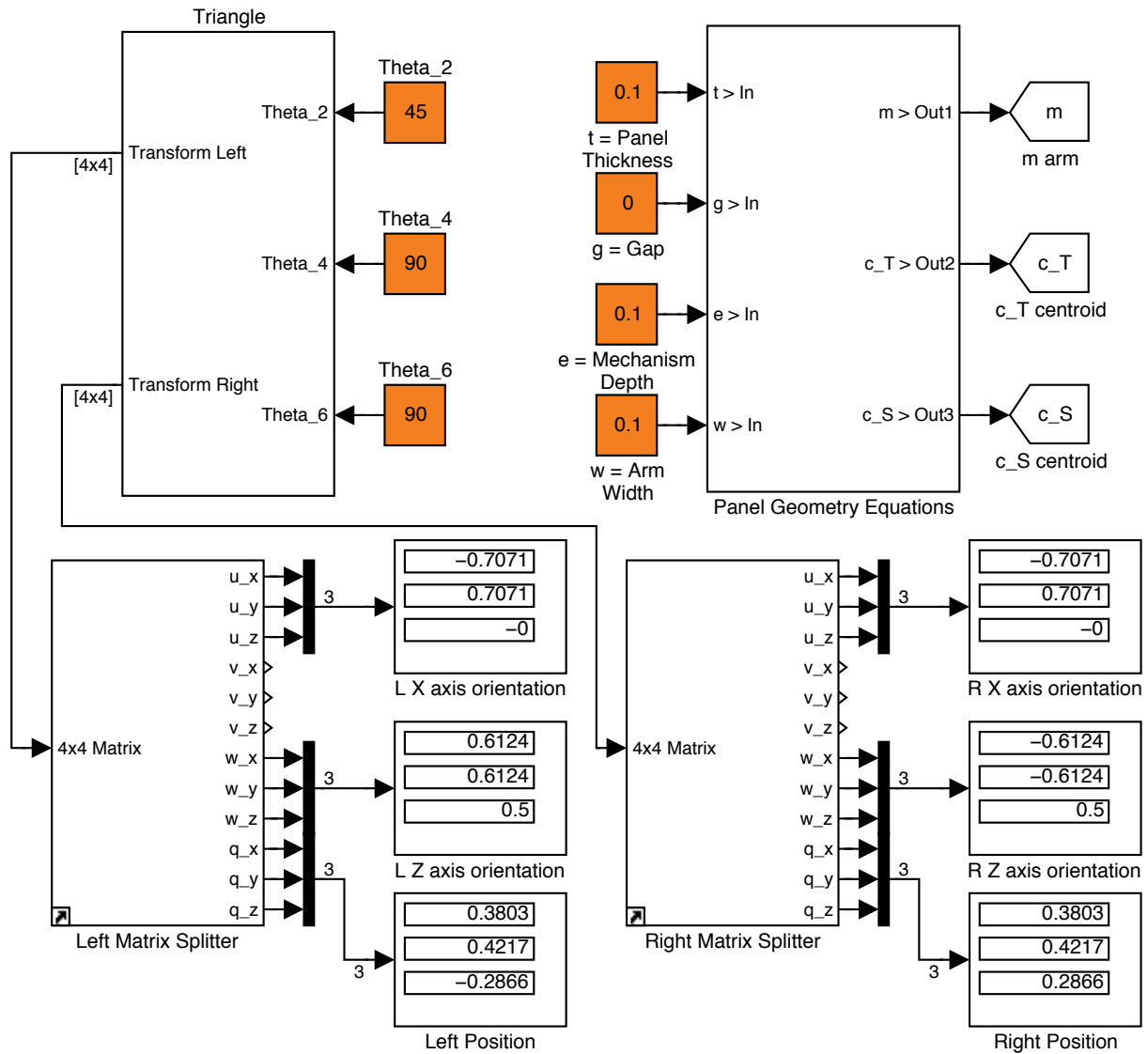


**Figure 10: Control panel for calculating triangle panel forward kinematics**

Similarly, Figure 11 shows a control panel for inputting final position and orientation vectors, and outputting the angle values for each of the joints.

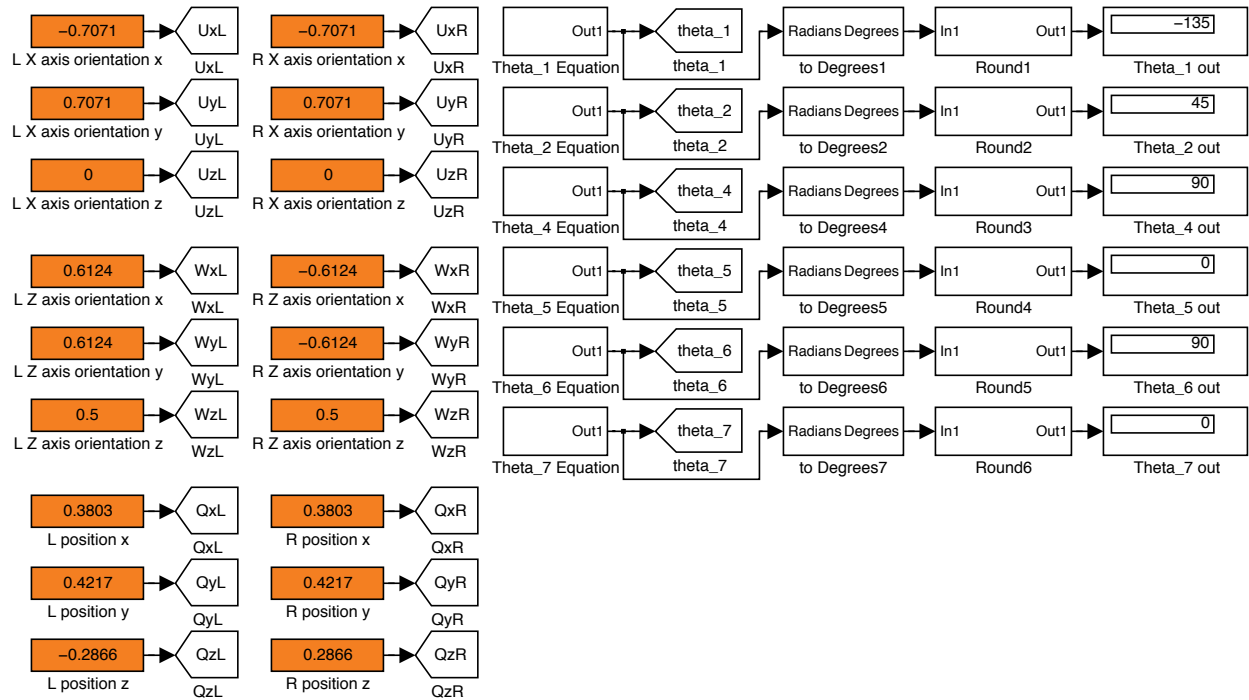


Figure 11: Control panel for calculating triangle panel inverse kinematics

#### IV. Mechanism Design Studies

Preliminary mechanism design concentrated on sliding internal housings for the connector arm manipulators. Initially, pneumatic linear actuators were used to test gearing, mechanism size, and kinematic performance. The internal housing for the connector arm rotation consists of the connector arm with electrical and data contacts, a pair of pneumatic cylinders, and gear boxes. Figure 12 shows the mechanism with attached pneumatic tubing.

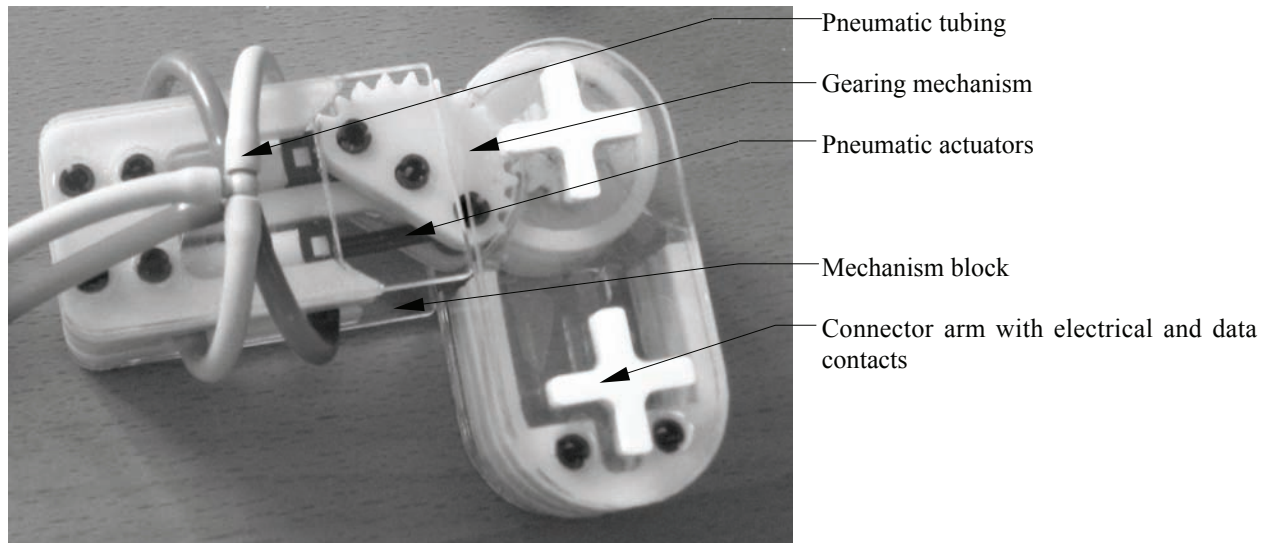
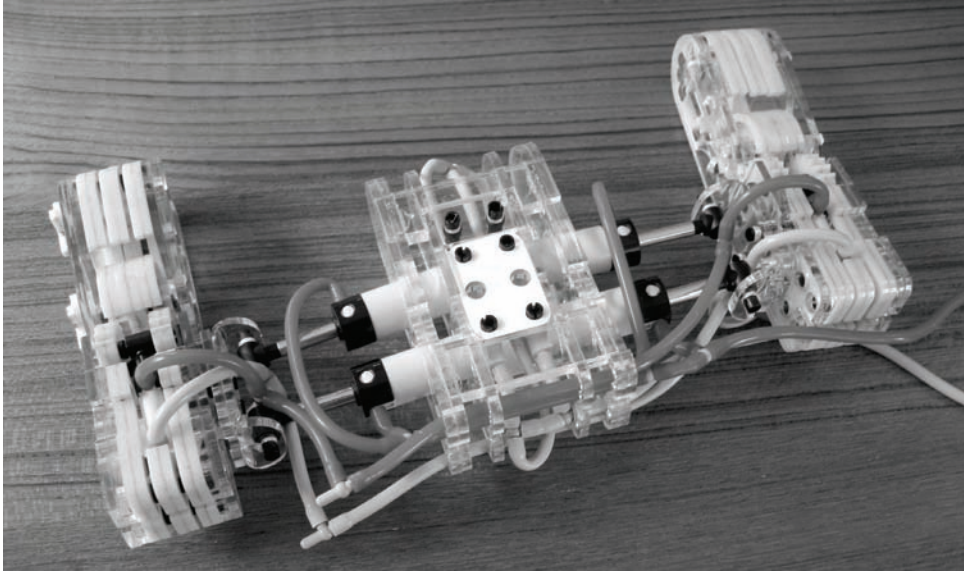
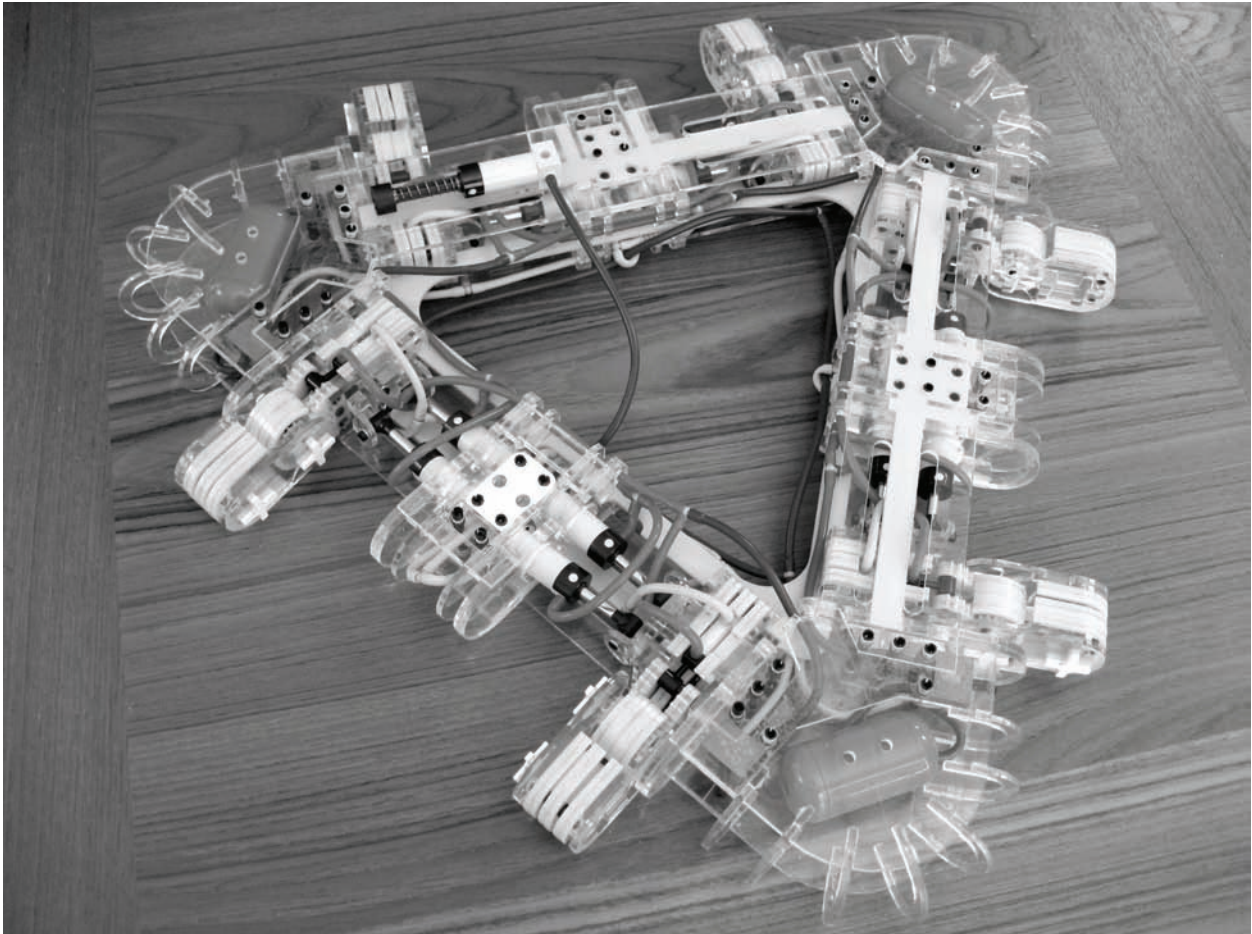


Figure 12: Sliding internal mechanism housing



**Figure 13: Connector arm and manipulator for one side**



**Figure 14: Kinematically functional triangle panel prototype**

Figure 13 shows a complete assembly of the functional connector arm and manipulator mechanism, with sliding internal mechanism housings on each side, and the prismatic manipulator mechanism in the middle. A fully

assembled triangle panel is shown in Figure 14. The triangle panel prototype was used to visualize the function of mechanism size, motion, and structure. The data from the initial prototype is being applied to a second-generation prototype using electrical actuators.

## V. Conclusion

Establishing a robust modular robotic construction system will build tremendous flexibility into orbital and planetary surface infrastructure. The Trigon robotic pairs can act as independent agents in a coordinated self-assembly of habitats and vehicles (Howe 2002, and Howe & Gibson 2006a). Figure 15 shows design studies for wheeled vehicles using the Trigon system.



**Figure 15: Pressurized rover constructed of Trigon panels and inflatable liner**

Payload panels inserted into the Trigon panel holes, drawing current and data from the panel itself, can provide the base structure for a variety of plug-in functionality, including mining implements, shielding, wheeled mobility, and cassette factories (Howe 2005).

## References

- C.D. Crane III; J. Duffy (1998). *Kinematic Analysis of Robot Manipulators*. Cambridge, UK: Cambridge University Press.
- A.S. Howe (2002). *The Ultimate Construction Toy: Applying Kit-of-Parts Theory to Habitat and Vehicle Design* (AIAA 2002-6116). 1st Space Architecture Symposium (SAS 2002), Houston, Texas, USA, 10-11 October 2002. Reston, Virginia, USA: American Institute of Aeronautics and Astronautics.
- A.S. Howe (2005). *Cassette Factories and Robotic Bricks: a Roadmap for Establishing Deep Space Infrastructures* (SAE 2005-01-2911). Proceedings of the 35th International Conference on Environmental Systems (ICES2005), 11-14 July 2005, Rome, Italy. 400 Commonwealth Drive, Warrendale, PA: Society of Automotive Engineers.
- A.S. Howe; I. Gibson (2006a). *MOBITAT2: A Mobile Habitat Based on the Trigon Construction System* (AIAA 2006-7337). 2nd International Space Architecture Symposium. San Jose, California, USA, 19-21 September 2006. Reston, Virginia, USA: American Institute of Aeronautics and Astronautics.
- A.S. Howe; I. Gibson (2006b). *Trigon Panel Size Optimization Studies* (AIAA 2006-7328). 2nd International Space Architecture Symposium. San Jose, California, USA, 19-21 September 2006. Reston, Virginia, USA: American Institute of Aeronautics and Astronautics.
- C.S.G. Lee (1983). *Robot Arm Kinematics*. In C.S.G. Lee, R.C. Gonzalez, and K.S. Fu (eds) (1983), *Tutorial on robotics*. Silver Spring, Maryland, USA: IEEE Computer Society Press. Pp. 47-65.

C.S.G. Lee (1983). Robot Arm Dynamics. In C.S.G. Lee, R.C. Gonzalez, and K.S. Fu (eds) (1983), Tutorial on robotics. Silver Spring, Maryland, USA: IEEE Computer Society Press. Pp. 93-102.

R.L. Norton (2004). Design of Machinery: An Introduction to the Synthesis and Analysis of Mechanisms and Machines, Third Edition. New York, NY, USA: McGraw-Hill.

R.P. Paul (1986). Robot Manipulators: Mathematics, Programming, and Control. Cambridge, Massachusetts, USA: The MIT Press.

R.P. Paul; B. Shimano; G.E. Mayer (1981). Kinematic Control Equations for Simple Manipulators. In C.S.G. Lee, R.C. Gonzalez, and K.S. Fu (eds) (1983), Tutorial on robotics. Silver Spring, Maryland, USA: IEEE Computer Society Press. Pp. 66-72.

L.W. Tsai (1999). Robot Analysis: the Mechanics of Serial and Parallel Manipulators. New York, NY, USA: John Wiley & Sons, Inc.

L.W. Tsai (2000). Mechanism Design: Enumeration of Kinematic Structures According to Function. CRC Press: Boca Raton, Florida.

### **Nomenclature**

*AIAA* = American Institute of Aeronautics and Astronautics  
*ISRU* = In-situ Resource Utilization  
*NASA* = National Aeronautics and Space Administration  
*Trigon* = Transformable Robotic Infrastructure-Generating Object Network system